Bioorganic & Medicinal Chemistry 20 (2012) 6248–6255

Contents lists available at SciVerse ScienceDirect

Bioorganic & Medicinal Chemistry

journal homepage: www.elsevier.com/locate/bmc

The antitumor agent doxorubicin binds to Fanconi anemia group F protein

Tomoe Kusayanagi [a], Senko Tsukuda [a], Satomi Shimura [a], Daisuke Manita [a], Kanako Iwakiri [b], Shinji Kamisuki [a], Yoichi Takakusagi [a], Toshifumi Takeuchi [a], Kouji Kuramochi [c], Atsuo Nakazaki [b], Kengo Sakaguchi [a], Susumu Kobayashi [b], Fumio Sugawara [a,*]

[a] Department of Applied Biological Science, Faculty of Science and Technology, Tokyo University of Science, 2641 Yamazaki, Noda, Chiba 278-8510, Japan
[b] Department of Medicinal and Life Science, Faculty of Pharmaceutical, Sciences, Tokyo University of Science, 2641 Yamazaki, Noda, Chiba 278-8510, Japan
[c] Graduate School of Life and Environmental Sciences, Kyoto Prefectural University, Sakyo-ku, Kyoto 606-8522, Japan

ARTICLE INFO

Article history:
Received 20 July 2012
Revised 6 September 2012
Accepted 7 September 2012
Available online 16 September 2012

Keywords:
Doxorubicin
Cisplatin
Fanconi anemia group F protein
Phage display
Mode of action

ABSTRACT

Doxorubicin, a commonly used cancer chemotherapy agent, elicits several potent biological effects, including synergistic-antitumor activity in combination with cisplatin. However, the mechanism of this synergism remains obscure. Here, we employed an improved T7 phage display screening method to identify Fanconi anemia group F protein (FANCF) as a doxorubicin-binding protein. The FANCF-doxorubicin interaction was confirmed by pull-down assay and SPR analysis. FANCF is a component of the Fanconi anemia complex, which monoubiquitinates D2 protein of Fanconi anemia group as a cellular response against DNA cross-linkers such as cisplatin. We observed that the monoubiquitination was inhibited by doxorubicin treatment.

1. Introduction

Doxorubicin (DOX) is commonly used to treat a wide range of cancers and works by DNA intercalation (Fig. 1).[1–3] Although the antitumor activity is highly effective in cancer therapy, single agent treatment with DOX generally induces a severe drug resistance in cancers. Hence, DOX is usually used in combination with other antitumor drugs as a multi-drug therapy to avoid the development of drug resistance.[4–6] The combination of drugs often shows a synergistic effect rather than an additive effect. A combination of DOX and cisplatin (CDDP), a DNA-crosslinking agent, has been commonly used and shows a synergistic effect.[7,8] However, the molecular mechanisms of this synergism remain obscure.

Several studies have reported that some drugs have multiple binding partners.[9,10] DOX exhibits cytotoxicity in cancer cells due to its interaction with the cell membrane and intercalation into the DNA.[2,11] Nucleolar phosphoprotein hNopp140, which is thought to act as a key component of nucleolus formation, has also been reported to be a DOX-binding partner.[9] Moreover, the phosphorylation of hNopp140 is reduced by DOX treatment.[12] However, these observations are insufficient in understanding the synergism against cancers by the combination of DOX and CDDP.

The phage display screening method is a powerful tool for identifying binding target(s) of a specific ligand.[13,14] However, the procedure is often laborious due to the occurrence of non-specific binding events combined with a complicated screening system. To overcome these problems, we recently reported an improved T7 phage display screening method that focuses on the identification of small-molecule-binding proteins.[15,16] In this method, a derivative of the small molecule under investigation is synthesized to form a self-assembled monolayer (SAM). The derivative is then immobilized on a gold electrode of a quartz-crystal microbalance (QCM) biosensor via thiol-gold interactions.[17] Peptides displayed on T7 phage particles that bind to the immobilized compound are subsequently selected from a T7 phage random peptide library. Obtained peptide sequences are analyzed with a Receptor Ligand Contacts (RELIC) bioinformatics program using a database of human proteins to identify putative protein binding partners for the small molecule.[18,19] This procedure has several advantages over other screening methods: (i) SAM reduces nonspecific binding, (ii) real-time monitoring of interaction is available, and (iii) analysis of peptides allows new binding candidates to be identified that cannot be obtained from a T7 phage cDNA library.[20]

In this study, we employed the improved phage display method to identify Fanconi anemia group F protein (FANCF) as a DOX binding protein candidate,[21] and confirmed the binding by pull-down assay and SPR analysis. FANCF is a component of a Fanconi anemia (FA) complex, which monoubiquitinates the D2 protein of Fanconi anemia group (FANCD2).[22,23] DNA-crosslinking agents such as CDDP induce the monoubiquitination of FANCD2 as a DNA repair response.[24] We showed that the monoubiquitination induced by

* Corresponding author. Tel.: +81 471 24 1501x3400; fax: +81 471 23 9767.
E-mail address: sugawara@rs.noda.tus.ac.jp (F. Sugawara).

0968-0896/$ - see front matter © 2012 Elsevier Ltd. All rights reserved.
http://dx.doi.org/10.1016/j.bmc.2012.09.015

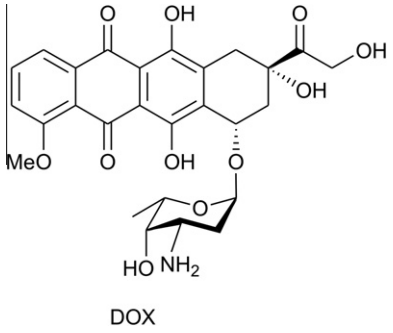

Figure 1. Structure of DOX.

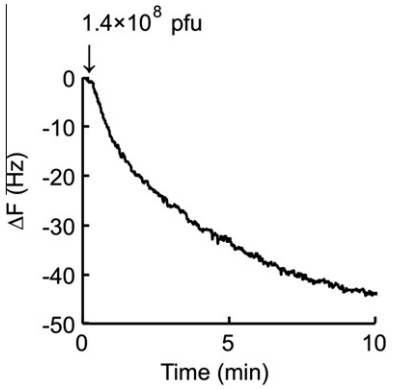

Figure 2. A representative sensorgram obtained by affinity selection of peptides on the QCM biosensor using DOX-SAM and T7 phage random peptide library. The DOX-SAM-immobilized sensor chip was first attached to the QCM biosensor. After injecting the T7 phage random peptide library at the indicated concentration, the frequency change was monitored for 10 min.

CDDP was inhibited by DOX treatment. Our results suggested that the DOX-FANCF binding might inhibit FANCD2 monoubiquitination.

2. Results

2.1. Screening of a T7 phage random peptide library against DOX-SAM

We synthesized DOX derivatives that form SAM on the gold electrode (DOX-SAM, **2**) for screening of a T7 phage random peptide library. DOX was converted into DOX-SAM (**2**) by coupling with 4-nitrophenyl carbamate **1**, which was prepared from amine salt (Scheme 1).[15] This compound contains the disulfide bound for chemisorption on the gold surface, a C11 alkyl chain for accumulation of the DOX molecule on the gold and diethylene glycol for reducing the non-specific binding (mainly via hydrophobic interactions).[25]

To identify DOX binding proteins, we employed an improved T7 phage display screening, which was reported in our previous work.[15] First, DOX-SAM was immobilized onto the gold electrode surface of a QCM sensor chip via thiol–gold interactions. The sensor was then fully stabilized in the QCM apparatus using a cuvette filled with a buffer solution. A T7 phage random peptide library displaying 15-mer randomized amino acids on the surface of their capsid structures was injected into the cuvette. Binding between DOX-SAM and phage particles was monitored by a frequency change in real-time (Fig. 2). After the interaction, the phage particles recognizing DOX on the gold electrode surface were recovered, and the displayed peptide sequences were determined by genome sequencing of the phage. We carried out five sets of independent screenings to obtain 27 different peptides that potentially recognize DOX (Table 1).

2.2. Identification of DOX-binding protein candidates using RELIC program

RELIC programs were developed to analyze interaction between bioactive compounds and peptides selected from phage libraries with affinities against compounds.[18] FASTAskan is one of the RELIC programs for calculating similarity scores between query peptides and a database of proteins. Proteins representing higher similarity scores are identified as candidate binding proteins of the compound of interest.

We obtained DOX-selected peptides by phage display screening. To identify DOX-binding protein candidates, we analyzed the peptides against the human IPI database (http://www.ebi.ac.uk) using the FASTAskan program (Supplementary Fig. 1). Among the top 10 proteins showing the highest similarity score, FANCF protein has a relationship with cisplatin sensitivity (Table 2).

FANCF is a component of the FANC-BRCA DNA repair pathway.[24,26] The pathway is required for the normal cellular response to DNA damage induced by UV radiation or chemicals, such as CDDP. Furthermore, FANCF has been reported as a possible determinant of CDDP resistance in cancer cells. Taniguchi et al. proposed a model for ovarian tumor progression in which the initial methylation

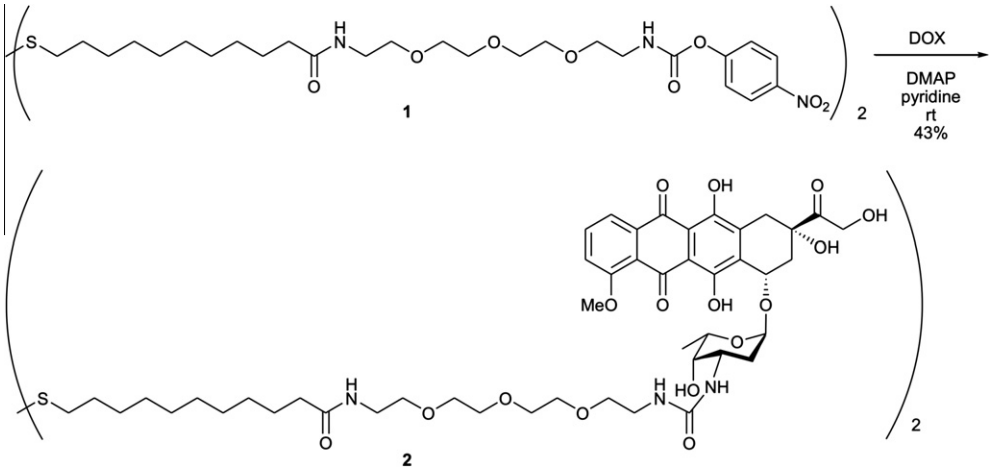

Scheme 1. Synthesis of DOX derivative to form SAM.

Table 1
DOX-SAM selected 15-mer peptide sequences. In total, 27 peptides were obtained after five sets of independent screenings

No.	Sequence	No.	Sequence	No.	Sequence
1	AASGRLVDVYNSCVS	10	GTICVCTFFCMVRCA	19	SCAVITYPSQDFNIS
2	CFCSCYGLIGQGDGV	11	ICTFQDLLVVQTVSD	20	SNLLWCVGRFSMYCD
3	CGYRQLSLFLTCPSE	12	IHVLSLQYNAAYVGT	21	VCCRLLWGYVLLFLL
4	CWCDGNLSNIDADLY	13	IYTCYIVVAWTFTVP	22	VCFVGVFPGMVNCDV
5	DAFTPLLGVRQMRRL	14	LCYIRVRDSRCLSYM	23	VFSGLVALRLPGCTS
6	FLLFVPQSIDHLNGG	15	LSFWTFAFASVRMLN	24	VSLGDCVSYCGLSIG
7	FSCLTHAVSLPITGS	16	LVYLCSSAALHNSDS	25	WLSGDFFGAVDLTVT
8	FWCALRHVGSDHPLW	17	PFIVHGFDCERFGLG	26	YDLLGVYRLSSRFAW
9	FYCFCIIAYLCNMGL	18	RSCVTLGCESWAVPR	27	YGHFIFLIVLFLFVC

Table 2
Summary of candidate DOX-binding proteins. The candidates are listed in order by similarity scores obtained from the FASTAskan program. The program ranked proteins in descending order of score, which was calculated from sequence similarity between DOX-selected peptides and proteins in the IPI human database

No.	Similarity score	Accession No.	Protein
1	295.82	IPI00174959.1	Isoform 1 of WD repeat-containing protein 81
2	295.82	IPI00163578.1	FLJ00182 (FRAGMENT)
3	286.38	IPI00294547.1	HLA class I histocompatibility antigen, alpha chain F [Precursor] (MHC class I antigen)
4	272.04	IPI00009290.1	Fanconi anemia group F protein (FANCF)
5	268.82	IPI00010575.2	KIAA1466 protein [Fragment]
6	262.96	IPI00018295.1	Splice isoform short of C-X-C chemokine receptor type 5
7	262.96	IPI00027955.1	Splice isoform long of C-X-C chemokine receptor type 5
8	260.69	IPI00152196.1	*N*-Acylneuraminate-9-phosphatase
9	259.68	IPI00167435.1	Zinc finger protein 781
10	247.31	IPI00335553.1	Similar to codanin I

of *FANCF* gene is followed by *FANCF* gene demethylation resulting in both FANCF expression and CDDP resistance.[27]

In this study, FANCF was identified as a candidate DOX-binding protein. Our findings, together with those of previous reports, suggest DOX may impair the function of FANCF through direct binding, which may explain why cancer cell death induced by CDDP is more effective in the presence of DOX. Hence, we focused on the molecular interaction between DOX and FANCF.

2.3. FANCF protein interacts with DOX

2.3.1. Pull-down assay

To investigate DOX-FANCF interaction by pull-down assay, we synthesized biotinylated DOX (DOX-Bio, **4**). DOX was coupled with succinimidyl 6-(biotinamido)hexanoate to afford DOX-Bio (**4**) (Scheme 2) and immobilized on an avidin agarose resin. Flag-tagged full-length FANCF protein (flag-FANCF) was expressed in human embryonic kidney (HEK) 293T cells. The cell lysates were then incubated with DOX-Bio-immobilized avidin agarose resin or non-immobilized control resin. After incubation, the two resins were washed and the bound flag-FANCF was detected by Western blotting using an anti-FANCF antibody. The amount of FANCF protein on DOX-Bio-immobilized resin was higher than that of the control resin (Fig. 3A), suggesting that DOX binds to FANCF.

2.3.2. Surface plasmon resonance analysis

Surface plasmon resonance (SPR) analysis was carried out to determine kinetic parameters of the DOX-FANCF interaction. DOX itself was immobilized on a sensor chip of an SPR biosensor (Biacore 3000) and then tested against various concentrations of recombinant FANCF protein. Our results showed that the binding between DOX and FANCF occurred in a dose-dependent manner (Fig. 3B, Table 3). The dissociation constant (K_D) of direct interaction between DOX and FANCF was determined to be 5.3×10^{-7} M, which is a relatively high affinity. Bovine serum albumin (BSA) as a negative control did not represent any binding against DOX in the same range of concentrations as that for calculation of the dissociation constant between FANCF and DOX (Supplementary Fig. 2).

2.4. Prediction of DOX-binding sites in the FANCF protein sequence

To predict DOX-binding sites in FANCF, DOX-selected peptides were used as input for a similarity-scanning program, MATCH of the RELIC program.[18,20] The program calculates cumulative similarity scores along the full length of the protein. Regions of the protein exhibiting the highest sequence similarity with the selected peptides represent potential ligand binding sites. The sequence of

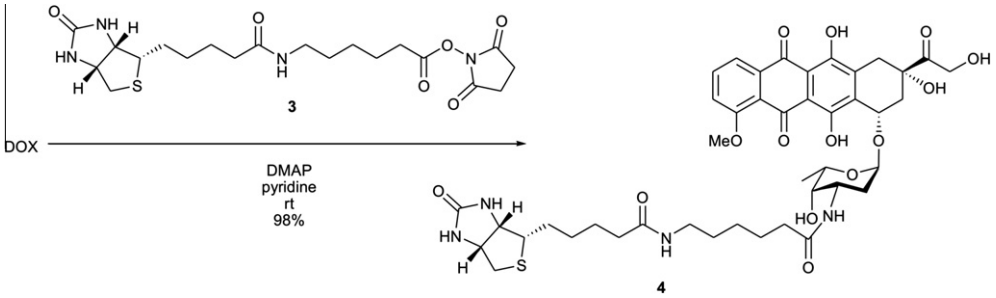

Scheme 2. Synthesis of the biotinylated DOX derivative.

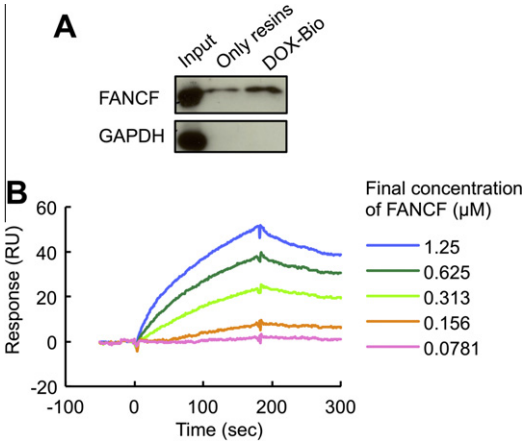

Figure 3. Binding analysis of recombinant FANCF with DOX. (A) Detection of FANCF binding to DOX by pull-down assay. Cell extracts of HEK293T cells overexpressing flag-FANCF were prepared and used for the assay. Proteins bound to DOX-Bio-immobilized avidin agarose resins were isolated and detected by Western blot analysis using anti-FANCF antibody (lane: DOX-Bio). As a control, proteins bound to avidin agarose resins were detected (lane: only resins). (B) An SPR analysis for the binding between DOX and FANCF. Analytes were injected over flow cells on the immobilized DOX. The background resulting from an injection of running buffer was subtracted from the data before plotting. Resonance units (RU) were generated by subtraction of the background signal generated simultaneously on the control flow cell.

Table 3
Summary of kinetic parameters of the interaction between DOX and FANCF calculated by BIAevaluation 4.1 software. k_a: association rate constant, k_d: dissociation rate constant, K_A: association constant, K_D: dissociation constant

k_a (M^{-1} s^{-1})	k_d (s^{-1})	K_A (M^{-1})	K_D (M)
6.5×10^3	1.8×10^{-3}	5.2×10^6	5.3×10^{-7}

FANCF was compared with the sequences of DOX-selected peptides and the resulting similarity plots exhibited four peaks; one near the N-terminal residue L14; a larger peak at residue L93; and a closely adjacent pair of peaks near residue L350, which is located in the C-terminus (Fig. 4A). Thus, these residues are predicted as possible DOX-binding sites. In addition, alignment of the selected peptides with the sequence of FANCF around L93, which exhibited the highest similarity score, identified the sequence 'VLLSLRLL' (red colored letters in Fig. 4B) as a candidate DOX-binding site.

DNA damage induced by cross-linking agents, such as CDDP, activates the Fanconi anemia-BRCA (FANC-BRCA) DNA repair pathway. In this pathway, FA complex, in which FANCF acts as a molecular adaptor, activates the monoubiquitination of FANCD2 (Fig. 5A). Mutations in the central region of FANCF (L209R and F251R) have been reported to inhibit the monoubiquitination of FANCD2.[28] Deletion mutants in each N- and C-terminal domain of FANCF, including L14 and G343, also exhibit defects in the assembly of the FA complex and the monoubiquitination of FANCD2.[28] As described above, possible DOX-binding sites in FANCF include amino acid residues that are important for FANCD2 monoubiquitination. Thus, DOX may inhibit monoubiquitination through its interaction with FANCF.

2.5. Inhibition of FANCD2 monoubiquitination by DOX

To investigate whether DOX inhibits the monoubiquitination, HeLa cells were either treated with CDDP alone or with a combination of CDDP and DOX, and the ubiquitination level of FANCD2 was then analyzed by Western blotting (Fig. 5B). Monoubiquitinated FANCD2 (FANCD2-L) and the corresponding unmodified form (FANCD2-S) can be discriminated by their electrophoretic mobility. We found that CDDP treatment elevated the level of monoubiquitinated FANCD2 in agreement with previous reports.[29] However, DOX treatment repressed the CDDP-induced monoubiquitination of FANCD2.

3. Discussion

A random peptide library for phage display screening possesses a high degree of diversity.[30,31] Theoretically a random peptide library contains the entire protein sequence information and, unlike a cDNA library or a cell lysate, is unaffected by levels of expression or protein stability. We applied phage display screening to obtain DOX-recognizing peptides from a random peptide library. Similarity calculations between DOX-selected peptides and the human protein database identified FANCF as a candidate DOX-binding partner. Moreover, an analysis of the DOX-selected peptides with the sequence of FANCF identified a possible DOX-binding site. Thus, the selection of ligand-recognizing peptides allows us to identify both the candidate binding protein and the likely ligand binding site within the protein sequence.[18,32]

FANCF is a component of the FANC-BRCA DNA repair pathway. In some ovarian tumor cell lines, the FANC-BRCA DNA repair pathway is disrupted by promoter methylation of *FANCF*.[27,33] FANCF expression caused by promoter demethylation recovers the pathway.[27] In this report, we observed direct binding between DOX and FANCF suggested by our phage display screenings. The results described in this study, together with those from previous reports, suggest that the DOX-FANCF interaction might inhibit the cellular activity of FANCF.

Similarity calculations between DOX-selected peptides and FANCF predicted that the C-terminal domain (CTD) and N-terminal region (NTR) of FANCF include possible DOX-binding sequences. The CTD and NTR of FANCF contribute to the assembly of the FA complex.[28,34,35] CTD of FANCF interacts with Fanconi anemia group G protein (FANCG).[28] Mutation within the CTD is known to disrupt the composition of the FA complex.[28] The NTR of FANCF engages in interaction with a subcomplex composed of Fanconi anemia group C and E protein (FANCC, FANCE).[34,35] Mutation within NTR disrupts the interaction of FANCF with FANCC and FANCE, resulting in the inhibition of assembly of the FA complex.[35] Thus, CTD and NTR of FANCF might form a DOX-binding region. Moreover, DOX-binding to these regions of FANCF may alter the composition of the FA complex and the downstream monoubiquitination.

Combination therapy of DOX with CDDP shows a synergistic effect. In this study, we observed that DOX inhibited the monoubiquitination of FANCD2 caused by a defense response against DNA damage induced by CDDP. Our findings suggest that DOX may increase the sensitivity of cancer cells to CDDP by inhibiting monoubiquitination through disturbance of the cellular activity of FANCF.

We determined the binding of DOX to FANCF and observed the effect of DOX treatment on the monoubiquitination of FANCD2. Further experiments are required to confirm whether the DOX-FANCF interaction directly affects the monoubiquitination. In addition, inhibitors of the monoubiquitination are expected to restore sensitivity against CDDP in cancer cells.[29] A less-toxic derivative of DOX, which maintains inhibition of the monoubiquitination, would be a valuable CDDP sensitizer.

4. Conclusion

We employed an improved phage display screening procedure to identify FANCF as a DOX-binding protein. The DOX–FANCF

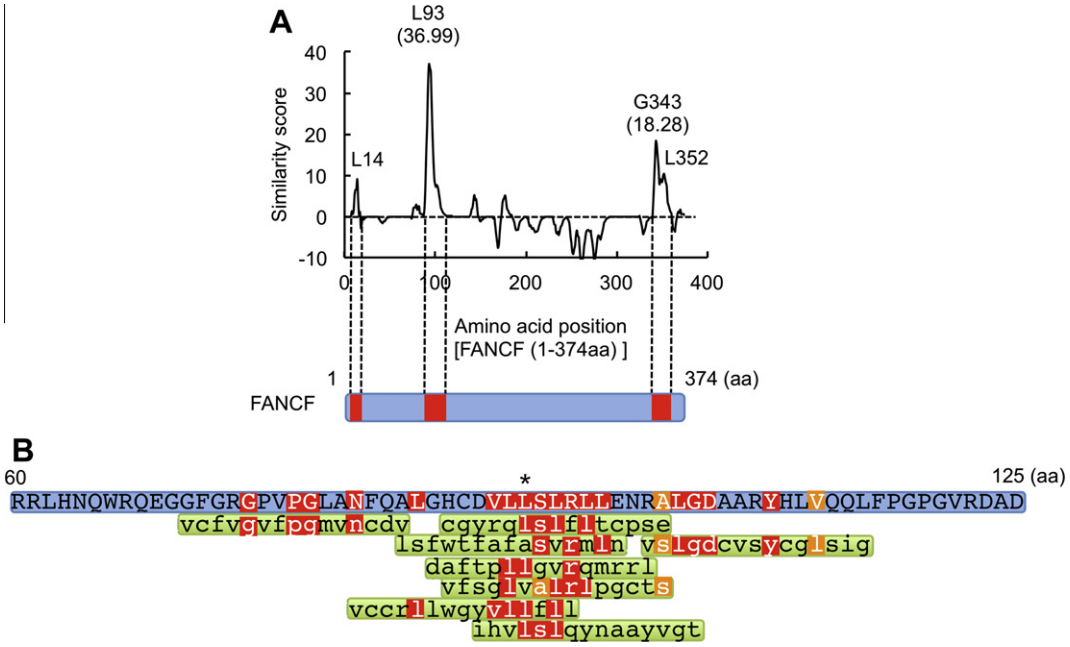

Figure 4. Similarity between DOX-selected peptides and FANCF. (A) Similarity scores between DOX-selected peptides and FANCF were obtained from the MATCH program. The scores were plotted against amino acid residues of FANCF. High similarity scores indicate that the DOX-selected peptides display a greater similarity to FANCF than randomly selected peptides. Negative similarity scores imply that DOX-selected peptides are less likely to have similarity to the regions than randomly selected peptides. Similarity scores in parentheses indicate significantly high scores. The blue bar represents full-length FANCF protein. Red parts indicate high similarity scores to DOX-selected peptides. (B) Alignment of FANCF (colored in blue) and DOX-selected peptides (in green) in region of highest similarity, which are obtained from the MATCH program. The red colored letters indicate identical residues and the orange colored letters indicate similar residues. The asterisk highlights Leu93, which displays the highest similarity score.

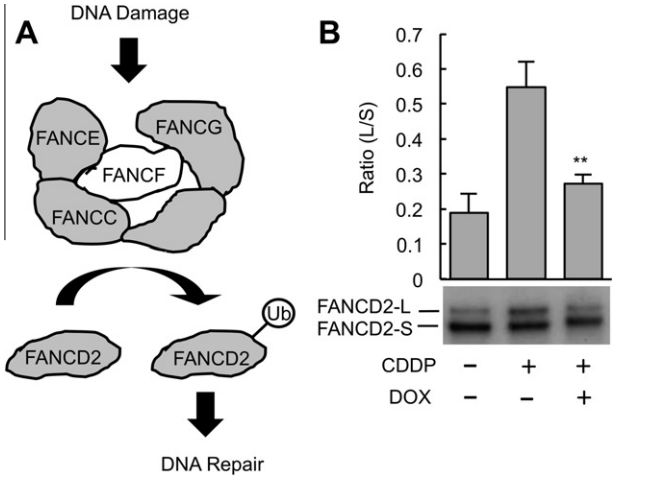

Figure 5. Inhibition of FANCD2 monoubiquitination by DOX. (A) Schematic model of the FANC-BRCA DNA repair pathway in which FANCF protein acts as a flexible adaptor protein. The pathway is required for the assembly of the Fanconi anemia (FA) complex. Monoubiquitination of FANCD2 is carried out by the FA complex. (B) Western blot analysis of FANCD2 monoubiquitination. HeLa cells were exposed to CDDP (0.9 μM) or a mixture of CDDP (0.9 μM) and DOX (9 μM) for 18 h. The whole cell lysates after incubation were examined by Western blotting using anti-FANCD2. FANCD2-S and FANCD2-L are the unmodified and monoubiquitinated forms of FANCD2, respectively. Densitometry was performed using ImageJ (National Institutes of Health, Bethesda, MD) to measure the ratio of FANCD2-L/FANCD2-S (L/S) is shown above the blots. $^{**}P < 0.01$ for CDDP and DOX-treated cells compared with CDDP only treated cells.

interaction was demonstrated by pull-down assay and SPR analysis. Furthermore, we observed that DOX inhibited the monoubiquitination of FANCD2, which is located downstream of FANCF. The DOX–FANCF interaction might disturb the cellular function of FANCF inhibiting the monoubiquitination of FANCD2. This monoubiquitination is required for CDDP resistance. Thus, DOX may increase cancer cell sensitivity against CDDP by inhibiting the monoubiquitination of FANCD2. Although, further experiments are required to confirm whether the DOX-FANCF interaction directly affects the monoubiquitination. We believe these studies may contribute to the research development of DOX-derivatives that can be more effective CDDP sensitizers than the parent compound.

5. Materials and methods

5.1. Synthesis of DOX derivatives

Doxorubicin hydrochloride was purchased from Tronto Research chemicals (Ontario, Canada). Biotinamidohexanoic acid *N*-hydroxysuccinimide ester was purchased from Sigma–Aldrich (St Louis, MO). All the other chemicals used for synthesis were purchased from Wako Pure Chemical Industries (Osaka, Japan).

^{1}H NMR spectra were recorded at 600 MHz on Bruker Avance DRX600 (Karlsruhe, Germany). Chemical Shifts (number of ^{1}H, multiplicity, *J* = coupling constants) were reported in delta (δ units in parts per million (ppm), relative to Me_4Si as an internal standard. Mass Spectra were obtained on ESI-MS spectrometer (API QSTAR pulsar i, AB SCIEX, Framingham, MA). Flash column chromatography was performed on silica gel PSQ 100B (Fuji Silysia Chemical Ltd, Aichi, Japan).

5.1.1. Bis(DOX-DEG-undecanyl) disulfide (2)

To a solution of DOX hydrochloride (4.6 mg, 7.9 μmol) and bis{10-{[11-(4-nitrophenoxycarbonylamino)-3,6,9-trioxaundecanyl]carbamoyl}undecanyl} disulfide (**1**) (3.8 mg, 3.4 μmol) in pyridine (1 mL) was added 4-(*N*,*N*-dimethylamino)pyridine (1.0 mg, 8.2 μmol) and the mixture was stirred at room temperature for 18 h. The solvent was removed by evaporation in vacuo and the

residue was purified on silca gel flash column chromatography (chloroform/methanol = 30:1 to 10:1) to give bis(DOX-DEG-undecanyl) disulfide (**2**) as a red waxy amorphous solid (2.8 mg, 43%). HRMS (ESI) *m/z* calcd for $C_{94}H_{132}N_6O_{32}Na_2S_2$ $[M+2Na]^{2+}$ 983.4056, found 983.4088 (error: 3.2 ppm); ^{1}H NMR (600 MHz, DMSO-d_6) δ 14.05 (2H, br s), 13.20 (2H, br s), 7.92–7.85 (2H, m), 7.74–7.68 (2H, m), 7.68–7.55 (4H, m), 6.05 (2H, t, J = 6.0 Hz), 5.78 (2H, d, J = 8.7 Hz), 5.41 (2H, br s), 5.21 (2H, br s), 4.94 (2H, dd, J = 4.2, 4.2 Hz), 4.79–4.77 (2H, br s), 4.71 (2H, brd, J = 6.0 Hz), 4.56 (4H, br s), 4.15–4.09 (2H, m), 3.96 (6H, s), 3.83–3.77 (2H, m), 3.49–3.43 (16H, m), 3.37–3.22 (10H, m), 3.14 (4H, m), 3.05 (4H, m), 2.97 (4H, s), 2.65 (4H, t, J = 7.2 Hz), 2.22–2.11 (4H, m), 2.01 (4H, t, J = 7.6 Hz), 1.72–1.64 (2H, m), 1.57 (4H, m), 1.51–1.46 (2H, m), 1.47–1.40 (4H, m), 1.34–1.27 (4H, m), 1.27–1.16 (20H, m), 1.12 (6H, d, J = 6.8 Hz).

5.1.2. N3′-[Biotynyl-6-aminohexanoyl]-DOX (4)

To a solution of DOX hydrochloride (5.4 mg, 9.3 μmol) in pyridine (2 mL) was added biotinamidohexanoic acid *N*-hydroxysuccinimide ester (**3**) (4.8 mg, 11 μmol) and 4-(*N*,*N*-dimethylamino)pyridine (0.9 mg, 7.4 μmol). The reaction mixture was stirred at room temperature for 16 h. The solvent was removed by evaporation in vacuo and the residue was purified on silica gel flash column chromatography (chloroform/methanol = 4:1) to afford N3′-[biotynyl-6-aminohexanoyl]-DOX (**4**) as a red waxy amorphous solid (8.1 mg, 98%). HRMS (ESI) *m/z* calcd for $C_{43}H_{54}N_4O_{14}NaS$ $[M+Na]^+$ 905.3249, found 905.3251 (error: 0.17 ppm); ^{1}H NMR (600 MHz, CD_3OD) δ 7.96 (1H, d, J = 8.0 Hz), 7.83 (1H, t, J = 8.1, 8.0 Hz), 7.56 (1H, d, J = 8.0 Hz), 5.41 (1H, d, J = 3.5 Hz), 5.14 (1H, s), 4.76 (1H, d, J = 19.9 Hz), 4.70 (1H, d, J = 19.9 Hz), 4.47–4.44 (1H, m), 4.28–4.24 (2H, m), 4.14–4.11 (1H, m), 4.02 (3H, s), 3.58 (1H, s), 3.15–3.08 (5H, m), 2.88 (1H, dd, J = 5.04, 12.7 Hz), 2.67 (1H, d, J = 12.7 Hz), 2.36 (1H, s), 2.20–2.11 (5H, m), 1.99–1.94 (1H, m), 1.69–1.64 (1H, m), 1.60–1.52 (6H, m), 1.48–1.43 (2H, m), 1.38–1.34 (2H, m), 1.32–1.28 (2H, m), 1.25 (3H, d, J = 6.5 Hz).

5.2. Construction of a T7 phage random peptide library

The library was constructed by using the T7Select 10-3b vector as outlined in the T7Select System Manual (Merck, Darmstadt, Germany). Random oligonucleotide insert DNA was synthesized in the following format: 5′-GGG GAT CCG AAT TCT-(NNK)$_{15}$-TGA AAG CTT CTC GAG GGG-3′, where N is A, C, G, or T (equimolar), and K is G or T (equimolar). The insert DNA was incubated with a complementary extension primer (5′-CCC TCG AGA AGC TTT CA-3′), Klenow DNA polymerase I (E.C. 2.7.7.7, USB, Cleveland, OH), and deoxyribonucleotide triphosphates (TaKaRa, Tokyo, Japan) to synthesize the complementary DNA strand. The reaction products were digested with EcoRI and HindIII restriction enzymes (E.C. 3.1.21.4, Merck), followed by phenol/chloroform extraction and ethanol precipitation using standard techniques. Then, the fragments were inserted into a T7select10-3b vector according to the manufacture's instructions.[36,37] The primary titer of this phage library was 1.6×10^7 pfu/mL. For the screening procedure, the phage library was amplified up to 1.7×10^{10} pfu/mL using *E. coli* (Rosetta-gami™ B5615) as a host strain.

5.3. Screening of the library

A 20 μL aliquot of DOX-SAM (1.3 mM in 75% ethanol) was dropped onto the gold electrode surface of the ceramic sensor chip and left for 16 h under a humid and shaded atmosphere at room temperature. After washing the sensor chip with ethanol and water, the chip was set up for the QCM apparatus (Affinix Q, Initium, Tokyo, Japan) with the cuvette containing 8 mL of screening buffer (10 mM Tris–HCl, 200 mM NaCl, pH 8.0). An 8-μL aliquot of T7 phage random peptide library was injected into the cuvette. Frequency changes, caused by phage binding to the DOX immobilized on the gold electrode surface, were then monitored for 10 min. The sensor chip was detached from the apparatus and air-dried. Bound phage particles were recovered by dropping 10 μL of host *E. coli* (BLT5615), which had been cultured for 30 min at 37 °C in the presence of 1 mM of isopropyl 1-thio-β-D-galactoside (IPTG) beforehand, onto the gold electrode of the sensor chip. The mixture of phages and *E. coli* was incubated at 37 °C for 30 min and the resulting solution was then removed and spread on Luria–Bertani agar plates supplemented with 50 μg/mL of carbenicillin (Nacalai Tesque, Kyoto, Japan). A total of 114 clones were randomly selected from the plates and each clone was dissolved in phage extraction solution (20 mM Tris–HCl, 100 mM NaCl, 6 mM $MgSO_4$, pH 8.0). An aliquot of phage was then extracted from this solution and subjected to PCR analysis followed by agarose gel electrophoresis and DNA sequencing for determination of the amino acid sequence displayed on the phage capsid.[15]

5.4. Bioinformatics tools

RELIC programs were used for the analyses of the obtained peptides from the phage library. DOX-binding candidates were identified with the FASTAskan program by using the selected peptide sequences as input against the human IPI database (http://www.ebi.ac.uk), which contained 57828 protein sequences. We used the MATCH program to locate potential DOX-binding sites in FANCF.

5.5. Cell lines and culture conditions

HeLa and HEK293T cells were maintained in Dulbecco's modified Eagle's medium supplemented with 10% fetal bovine serum, 100 units/mL penicillin, and 100 μg/mL streptomycin sulfate at 37 °C under an atmosphere of 5% CO_2.

5.6. Vector constructions

To generate flag-tagged full-length FANCF protein (flag-FANCF), *FANCF* cDNA was PCR amplified from a cDNA library of human thymus using primers containing suitable restriction sites and ligated into the HindIII and BamHI restriction sites of pFLAG-CMV-4 (Sigma–Aldrich). To generate histidine- and trigger factor-tagged FANCF protein (His-TF-FANCF), FANCF cDNA was PCR-amplified from a cDNA library of human thymus using primers containing suitable restriction sites and ligated into the NdeI and XhoI restriction sites of pCold TF DNA (TaKaRa).

5.7. Pull-down assay

HEK293T cells expressing flag-FANCF were generated by transfecting pFLAG-CMV4 based vector and harvested into 1 mL of phosphate-buffered saline (PBS: 67 mM Na_2HPO_4, 12.5 mM KH_2PO_4, 70 mM NaCl, 1 mM DTT, 1% DMSO, pH 7.4). The recovered cells were then sonicated and centrifuged at 20,400×g for 1 min. The supernatants (2 mg total protein, 1 mL) were taken and used for a pull-down assay with 10 μL of DOX-Bio immobilized avidin agarose or control avidin agarose resin (Sigma–Aldrich). After mixing overnight, the resins were washed three times with PBS and mixed with SDS loading buffer (0.002% bromophenol blue, 0.002% xylene cyanol FF, 5% glycerol, 0.1% SDS) and incubated at 95 °C for 10 min. After centrifugation at 20,400×g for 1 min, the

supernatants were subjected to SDS–PAGE using a 10% polyacrylamide gel. The separated proteins were blotted onto a PVDF membrane and FANCF protein was detected by Western blot analysis using anti-FANCF (Abcam, Cambridge, MA) as a primary antibody and HRP-coupled anti-rabbit (Sigma–Aldrich) as a secondary antibody.

5.8. Expression and purification of FANCF protein

Full length FANCF protein was expressed as a histidine- and trigger factor-tagged FANCF protein (His-TF-FANCF) using a pCold TF DNA. Rosetta™ 2(DE3) pLysS cells (Merck) were induced with 1 mM IPTG for 24 h, 15 °C. The cells were sonicated in sonication buffer [0.5 M NaCl, 8.10 mM Na_2HPO_4, 2.68 mM KCl, 1.47 mM KH_2PO_4, 0.005% (w/v) Triton X-100, 0.5% (w/v) glycerol, pH 7.4] with a protease inhibitor cocktail (EDTA free) (Nacalai Tesque). The cleared cell supernatant prepared by centrifugation was then passed through a 1 mL HisTrap HP column (GE Healthcare, Waukesha, WI). The bound proteins on the column were washed with sonication buffer solution and subsequently eluted using a gradient of imidazole (0–500 mM) in the same buffer solution. The fractions containing the His-TF-FANCF protein were collected. A solution of 1 mg of His-TF-FANCF in 1.5 mL was incubated with 60 U of HRV 3C protease (Merck) at 4 °C for 16 h in order to remove the His-TF tag. The buffer used for the digest was exchanged with binding buffer [0.5 M NaCl, 8.10 mM Na_2HPO_4, 2.68 mM KCl, 1.47 mM KH_2PO_4, 0.5 M arginine, 5 mM DTT, 0.05% (w/v) Triton X-100, 0.5% (w/v) glycerol, pH 7.4]. The resulting solution was applied to a 1 mL HisTrap HP column to which the protease bound. Cleaved FANCF was recovered from the flow-through fraction. The buffer in the FANCF fraction was exchanged to PBS-T [0.5 M NaCl, 8.10 mM Na_2HPO_4, 2.68 mM KCl, 1.47 mM KH_2PO_4, 1 mM DTT, 0.05% (w/v) Triton X-100, 0.5% (w/v) glycerol, pH 7.4] for SPR analysis.

5.9. Surface plasmon resonance

The binding kinetics of DOX and the FANCF protein were analyzed using the Biacore 3000 instrument (GE Healthcare). DOX was immobilized onto a sensor chip CM5, typically between 10 and 50 RU, using an amine coupling kit (GE Healthcare). Different concentrations of the FANCF protein in PBS-T were injected for 120 s at a flow rate of 20 μL/min. BIAevaluation 4.1 software was used to determine the kinetic parameters. The binding between DOX and BSA (Wako, Osaka, Japan) was analyzed in the same manner.

5.10. Detection of monoubiquitinated FANCD2

HeLa cells were seeded at 50–70% confluency. After 18-h of incubation with CDDP (0.9 μM) and DOX (9 μM), cells were lysed for 20 min at 4 °C in lysis buffer [50 mM Tris–HCl (pH 7.4), 150 mM NaCl, 1% (w/v) Triton X-100] supplemented with a protease inhibitor cocktail (EDTA free) (Nacalai Tesque). The lysates were cleared by centrifugation at 15,000×*g* for 20 min. Total protein concentrations for the supernatant were measured by the DC protein assay (Bio-Rad, Richmond, CA) and then normalized. The solutions were mixed with 4 × NuPAGE LDS Sample Buffer (Invitrogen, Carlsbad, CA) boiled for 10 min and subjected to SDS–PAGE in a 3–8% gradient gel (Invitrogen). The separated proteins were blotted onto a PVDF membrane and FANCD2 proteins were detected by Western blot analysis using anti-FANCD2 (Novus Biologicals, Littleton, CO) as a primary antibody and HRP-coupled anti-rabbit (GE Healthcare) as a secondary antibody. Enhanced chemiluminescence was used for detection.

Acknowledgments

We thank L. Makowski (Northeastern University) for supporting the RELIC analyses. This work was supported by Grant-in-Aid for JSPS Fellows (22·6175) (to T.K.).

Supplementary data

Supplementary data associated with this article can be found, in the online version, at http://dx.doi.org/10.1016/j.bmc.2012.09.015.

References

1. Carter, S. K.; Blum, R. H. *CA-Cancer J. Clin.* **1974**, *24*, 322.
2. D'Arpa, P.; Liu, L. F. *Biochim. Biophys. Acta* **1989**, *989*, 163.
3. Frederick, C. A.; Williams, L. D.; Ughetto, G.; van der Marel, G. A.; van Boom, J. H.; Rich, A.; Wang, A. H. *Biochemistry* **1990**, *29*, 2538.
4. Hoogstraten, B.; George, S. L.; Samal, B.; Rivkin, S. E.; Costanzi, J. J.; Bonnet, J. D.; Thigpen, T.; Braine, H. *Cancer* **1976**, *38*, 13.
5. Tranum, B.; Hoogstraten, B.; Kennedy, A.; Vaughn, C. B.; Samal, B.; Thigpen, T.; Rivkin, S.; Smith, F.; Palmer, R. L.; Costanzi, J.; Tucker, W. G.; Wilson, H.; Maloney, T. R. *Cancer* **1978**, *41*, 2078.
6. Aapro, M. S.; van Wijk, F. H.; Bolis, G.; Chevallier, B.; van der Burg, M. E.; Poveda, A.; de Oliveira, C. F.; Tumolo, S.; Scotto di Palumbo, V.; Piccart, M.; Franchi, M.; Zanaboni, F.; Lacave, A. J.; Fontanelli, R.; Favalli, G.; Zola, P.; Guastalla, J. P.; Rosso, R.; Marth, C.; Nooij, M.; Presti, M.; Scarabelli, C.; Splinter, T. A.; Ploch, E.; Beex, L. V.; ten Bokkel Huinink, W.; Forni, M.; Melpignano, M.; Blake, P.; Kerbrat, P.; Mendiola, C.; Cervantes, A.; Goupil, A.; Harper, P. G.; Madronal, C.; Namer, M.; Scarfone, G.; Stoot, J. E.; Teodorovic, I.; Coens, C.; Vergote, I.; Vermorken, J. B. *Ann. Oncol.* **2003**, *14*, 441.
7. Thigpen, J. T.; Brady, M. F.; Homesley, H. D.; Malfetano, J.; DuBeshter, B.; Burger, R. A.; Liao, S. *J. Clin. Oncol.* **2004**, *22*, 3902.
8. Lee, S. M.; O'Halloran, T. V.; Nguyen, S. T. *J. Am. Chem. Soc.* **2010**, *132*, 17130.
9. Jin, Y.; Yu, J.; Yu, Y. G. *Chem. Biol.* **2002**, *9*, 157.
10. Manita, D.; Toba, Y.; Takakusagi, Y.; Matsumoto, Y.; Kusayanagi, T.; Takakusagi, K.; Tsukuda, S.; Takada, K.; Kanai, Y.; Kamisuki, S.; Sakaguchi, K.; Sugawara, F. *Bioorg. Med. Chem.* **2011**, *19*, 7690.
11. Tritton, T. R.; Yee, G. *Science* **1982**, *217*, 248.
12. Kim, Y. K.; Lee, W. K.; Jin, Y.; Lee, K. J.; Jeon, H.; Yu, Y. G. *J. Biochem. Mol. Biol.* **2006**, *39*, 774.
13. Smith, G. P.; Petrenko, V. A. *Chem. Rev.* **1997**, *97*, 391.
14. Shim, J. S.; Lee, J.; Park, H. J.; Park, S. J.; Kwon, H. *J. Chem. Biol.* **2004**, *11*, 1455.
15. Takakusagi, Y.; Kuramochi, K.; Takagi, M.; Kusayanagi, T.; Manita, D.; Ozawa, H.; Iwakiri, K.; Takakusagi, K.; Miyano, Y.; Nakazaki, A.; Kobayashi, S.; Sugawara, F.; Sakaguchi, K. *Bioorg. Med. Chem.* **2008**, *16*, 9837.
16. Nishiyama, K.; Takakusagi, Y.; Kusayanagi, T.; Matsumoto, Y.; Habu, S.; Kuramochi, K.; Sugawara, F.; Sakaguchi, K.; Takahashi, H.; Natsugari, H.; Kobayashi, S. *Bioorg. Med. Chem.* **2009**, *17*, 195.
17. Schlenoff, J. B.; Li, M.; Ly, H. *J. Am. Chem. Soc.* **1995**, *117*, 12528.
18. Mandava, S.; Makowski, L.; Devarapalli, S.; Uzubell, J.; Rodi, D. J. *Proteomics* **2004**, *4*, 1439.
19. Miyano, Y.; Tsukuda, S.; Sakimoto, I.; Takeuchi, R.; Shimura, S.; Takahashi, N.; Kusayanagi, T.; Takakusagi, Y.; Okado, M.; Matsumoto, Y.; Takakusagi, K.; Takeuchi, T.; Kamisuki, S.; Nakazaki, A.; Ohta, K.; Miura, M.; Kuramochi, K.; Mizushina, Y.; Kobayashi, S.; Sugawara, F.; Sakaguchi, K. *Bioorg. Med. Chem.* **2012**, *20*, 3985.
20. Rodi, D. J.; Agoston, G. E.; Manon, R.; Lapcevich, R.; Green, S. J.; Makowski, L. *Comb. Chem. High Throughput Screening* **2001**, *4*, 553.
21. de Winter, J. P.; Rooimans, M. A.; van der Weel, L.; van Berkel, C. G.; Alon, N.; Bosnoyan-Collins, L.; de Groot, J.; Zhi, Y.; Waisfisz, Q.; Pronk, J. C.; Arwert, F.; Mathew, C. G.; Scheper, R. J.; Hoatlin, M. E.; Buchwald, M.; Joenje, H. *Nat. Genet.* **2000**, *24*, 15.
22. D'Andrea, A. D.; Grompe, M. *Nat. Rev. Cancer* **2003**, *3*, 23.
23. Thompson, L. H. *Nat. Genet.* **2005**, *37*, 921.
24. Garcia-Higuera, I.; Taniguchi, T.; Ganesan, S.; Meyn, M. S.; Timmers, C.; Hejna, J.; Grompe, M.; D'Andrea, A. D. *Mol. Cell* **2001**, *7*, 249.
25. Furuya, M.; Haramura, M.; Tanaka, A. *Bioorg. Med. Chem.* **2006**, *14*, 537.
26. Medhurst, A. L.; Huber, P. A.; Waisfisz, Q.; de Winter, J. P.; Mathew, C. G. *Hum. Mol. Genet.* **2001**, *10*, 423.
27. Taniguchi, T.; Tischkowitz, M.; Ameziane, N.; Hodgson, S. V.; Mathew, C. G.; Joenje, H.; Mok, S. C.; D'Andrea, A. D. *Nat. Med.* **2003**, *9*, 568.
28. Kowal, P.; Gurtan, A. M.; Stuckert, P.; D'Andrea, A. D.; Ellenberger, T. *J. Biol. Chem.* **2007**, *282*, 2047.
29. Chirnomas, D.; Taniguchi, T.; de la Vega, M.; Vaidya, A.; Vasserman, M.; Hartman, A. R.; Kennedy, R.; Foster, R.; Mahoney, J.; Seiden, M. V.; D'Andrea, A. D. *Mol. Cancer Ther.* **2006**, *5*, 952.
30. Devlin, J. J.; Panganiban, L. C.; Devlin, P. E. *Science* **1990**, *249*, 404.
31. Molek, P.; Strukelj, B.; Bratkovic, T. *Molecules* **2011**, *16*, 857.

32. Rodi, D. J.; Janes, R. W.; Sanganee, H. J.; Holton, R. A.; Wallace, B. A.; Makowski, L. *J. Mol. Biol.* **1999**, *285*, 197.
33. Wang, Z.; Li, M.; Lu, S.; Zhang, Y.; Wang, H. *Cancer Biol. Ther.* **2006**, *5*, 256.
34. Pace, P.; Johnson, M.; Tan, W. M.; Mosedale, G.; Sng, C.; Hoatlin, M.; de Winter, J.; Joenje, H.; Gergely, F.; Patel, K. J. *EMBO J.* **2002**, *21*, 3414.
35. Léveillé, F.; Blom, E.; Medhurst, A. L.; Bier, P.; Laghmani, E. H.; Johnson, M.; Rooimans, M. A.; Sobeck, A.; Waisfisz, Q.; Arwert, F.; Patel, K. J.; Hoatlin, M. E.; Joenje, H.; de Winter, J. P. *J. Biol. Chem.* **2004**, *279*, 39421.
36. Merck. *T7Select® System Manual*, 2000, TB178.
37. Merck. *OrientExpress*™ cDNA Manual, 1999, TB247.